Paper Number 2001-01-2793

Design of an Advanced Heavy Tactical Truck: A Target Cascading Case Study

Nestor Michelena, Loucas Louca, Michael Kokkolaras, Chan-Chiao Lin, Dohoy Jung, Zoran Filipi, Dennis Assanis, Panos Papalambros, Huei Peng and Jeff Stein
The University of Michigan

Mark Feury
U.S. Army Tank-automotive and Armaments Command – Tank Automotive Research, Development and Engineering Center

ABSTRACT

The target cascading methodology is applied to the conceptual design of an advanced heavy tactical truck. Two levels are defined: an integrated truck model is represented at the top (vehicle) level and four independent suspension arms are represented at the lower (system) level. Necessary analysis models are developed, and design problems are formulated and solved iteratively at both levels. Hence, vehicle design variables and system specifications are determined in a consistent manner. Two different target sets and two different propulsion systems are considered. Trade-offs between conflicting targets are identified. It is demonstrated that target cascading can be useful in avoiding costly design iterations late in the product development process.

INTRODUCTION

Target cascading is a key challenge in early product development stages of complex products: How to propagate desirable product characteristics, defined by product's specifications, to the various subsystems and components in a consistent and efficient manner. Consistency means that all parts of the designed system should end up working well together, while efficiency means that the process itself should avoid iterations at later stages, when they are more costly in terms of time and resources.

Analytical target cascading is formalized in a process modeled as a multilevel optimal design problem. Design targets are cascaded down to lower levels by partitioning the overall design problem into a hierarchical set of subproblems. For each design subproblem at a given level, a rigorous optimization problem is formulated to minimize deviations from the propagated targets and thus achieve intersystem compatibility. A coordination strategy links all subproblem decisions so that overall product performance targets are met.

The analytical target cascading methodology is applied to the design of an advanced heavy tactical truck. Novel technologies (e.g., series hybrid and electric propulsion systems, in-hub motors, and variable height suspensions) are introduced with the intention of improving both civilian and military design attributes within the framework of a dual-use philosophy. Emphasis is given to fuel economy, ride, and mobility characteristics. A two-level target cascading hierarchy is defined, and five design subproblems are formulated. At the top level, design targets for the truck are matched. At the bottom level, suspension characteristics, cascaded down from the top level, are matched using a detailed model of the suspension system.

Models were developed to simulate the transient response of both a series hybrid and an electric-driven truck at the top (vehicle) level, and the response of variable height suspensions at the bottom (system) level. The models at both the vehicle and system levels were tailored to fit the target cascading process. Automated modeling techniques were used to develop vehicle dynamics models that are computationally efficient, accurate, and described by physical parameters. Baseline designs were chosen to be consistent with vehicle concepts of the U.S. Army, whereas vehicle targets were defined to improve on the performance of existing designs. Design studies were performed for both series hybrid and series electric drive propulsion systems. Results are presented for two sets of targets.

The paper is organized as follows: The target cascading methodology is introduced in the next section. The vehicle description is then given, and the developed models necessary for the case study are presented. Implementation issues of the analytical target cascading process are then addressed, followed by the discussion of results. Conclusions are drawn in the last section of the paper.

TARGET CASCADING FOR VEHICLE DESIGN

Analytical target cascading entails a hierarchical decomposition of the product and the underlying models into systems, subsystems and components—called the elements. That is, it is assumed the product is made up of systems, the systems are made up of subsystems, and so on. Analytical or computational models are used to predict the behavior or response of the different elements; specifically, an element's response **R** is a function of the element's own design parameters and variables **x** as well as of the responses of (sub)elements making up the element. For example, powertrain system responses will depend on design parameters and variables inherent to the powertrain system as well as on the responses of the engine and drivetrain subsystems.

For each level and for each element in the model hierarchy, a design optimization problem is formulated to match responses dictated by elements above in the hierarchy and to satisfy the element's design constraints. The analytical target cascading formulation is general enough to account for multiple levels and for interactions between elements at the same level by means of linking design variables. In this article, we present a formulation for a two-level hierarchy (vehicle and systems) without linking design variables. That is, it is assumed that systems are not decomposable into subsystem and components and systems do not share design variables among themselves.[1]

VEHICLE-LEVEL DESIGN PROBLEM

At the vehicle level, responses $\mathbf{R}_v$ must match desired design specifications $\mathbf{T}_v$. These responses are assumed to be functions of vehicle design variables $\mathbf{x}_v$ and system responses $\mathbf{R}_{s_i}$, for $i = 1,\ldots,n_s$ systems, i.e., $\mathbf{R}_v = \mathbf{r}_v(\mathbf{x}_v, \mathbf{R}_{s_1},\ldots, \mathbf{R}_{s_{ns}})$. To determine target values for system responses $\mathbf{R}_{s_i}$ and vehicle design variables $\mathbf{x}_v$ a minimum deviation optimization problem is formulated as follows:

$$\text{Min} \quad \left\|\mathbf{R}_v - \mathbf{T}_v\right\| + \varepsilon_v^R$$

with respect to

$$\mathbf{x}_v, \mathbf{R}_{s_1}, \cdots, \mathbf{R}_{s_{n_s}}, \varepsilon_v^R$$

subject to

$$\sum_{i=1}^{n_s} \left\|\mathbf{R}_{s_i} - \mathbf{R}_{s_i}^L\right\| \le \varepsilon_v^R$$

$$\mathbf{g}_v(\mathbf{R}_v, \mathbf{x}_v) \le 0$$

$$\mathbf{h}_v(\mathbf{R}_v, \mathbf{x}_v) \le 0$$

where $\mathbf{x}_v$ is the vector of design variables exclusively associated with the vehicle, $\mathbf{R}_v$ is the vector of vehicle responses, $\mathbf{R}_{s_i}$—is the vector of responses for the *i-th* system making up the vehicle, ε_v^R is a tolerance variable for coordinating system responses, $\mathbf{T}_v$ is the vector of vehicle design targets or specifications, $\mathbf{R}_{s_i}^L$ is the vector of system response values passed up to the vehicle from the *i-th* system, and $\mathbf{g}_v$ and $\mathbf{h}_v$ are vector functions representing vehicle design constraints.

SYSTEM-LEVEL DESIGN PROBLEM

Once the optimal values of the system level responses $\mathbf{R}_{s_i}$, $i = 1,\ldots,n_s$, are determined by solving the vehicle-level design problem shown above, they are cascaded down to the system level as target values $\mathbf{R}_{s_i}^U$. At the system level, n_s individual minimum deviation optimization problems are formulated to determine the system design variables $\mathbf{x}_{s_i}$. System responses are assumed to be functions of system design variables alone, i.e., $\mathbf{R}_{s_i} = \mathbf{r}_{s_i}(\mathbf{x}_{s_i})$, given the two-level hierarchy assumption. The minimum deviation optimization problems for the $i = 1,\ldots,n_s$ systems are formulated as follows:

$$\text{Min} \quad \left\|\mathbf{R}_{s_i} - R_{s_i}^U\right\|$$

with respect to

$$\mathbf{x}_{s_i}$$

subject to

$$\mathbf{g}_{s_i}(\mathbf{R}_{s_i}, \mathbf{x}_{s_i}) \le 0$$

$$\mathbf{h}_{s_i}(\mathbf{R}_{s_i}, \mathbf{x}_{s_i}) \le 0$$

The analytical target cascading process iterates between the vehicle- and system-level design problems. At each iteration, values of $\mathbf{R}_{s_i}^L$ and $\mathbf{R}_{s_i}^U$ determined at the system- and vehicle-levels, respectively, are passed up and down to the other level design problem(s).

VEHICLE DESCRIPTION AND MODELING

A heavy tactical truck is selected in this article to demonstrate the implementation of the target cascading process. The vehicle is based on a new concept design aimed at improving the performance of its predecessor under the same operation conditions. This is the first attempt to use modeling and simulation to study the behavior of this vehicle. Fuel economy, mobility, and ride quality are identified as the critical characteristics that the new design must improve or at least maintain. Models that can accurately predict these characteristics were developed.

The vehicle has a series hybrid electric configuration with in-hub motors at all eight wheels. The driving power comes from a diesel engine and the battery modules. A new technology that is also employed in this vehicle is the trailing arm variable height suspension that provides high ground clearance for off road driving conditions. A schematic of the vehicle configuration is shown in Figure 1. Left and right tires are combined into one tire because of symmetry.

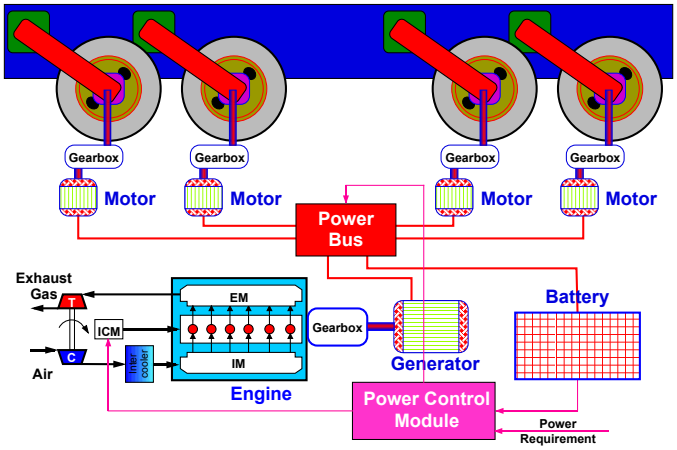

Figure 1. Vehicle model configuration

The vehicle is powered by a diesel engine that is connected to the generator through a speed reduction gearbox. The electrical power of the generator, through the power bus, is fed to eight in-hub motors that drive the wheels through a gearbox at each wheel. Additional power may be taken from the battery modules connected to the power bus. Distribution of power and charging and discharging of the batteries are managed by the power control module based on instantaneous power requirements.

For target cascading, the models are decomposed into an integrated vehicle model at the top level and four copies of a suspension system model at the low level, as shown in Figure 2. The top-level vehicle model predicts the vehicle responses $\mathbf{R}_v$, whereas the suspension model predicts the system responses $\mathbf{R}_{s_i}$, i = 1, 2, 3, 4.

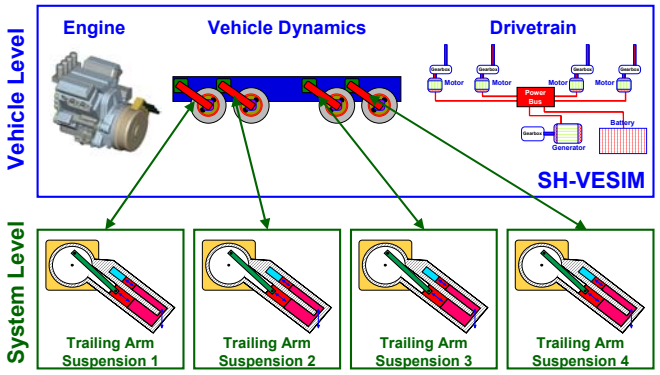

Figure 2. Hierarchy of models for target cascading

The basis for our top level, integrated Series Hybrid Vehicle-Engine SIMulation (SH-VESIM) was the high-fidelity conventional vehicle simulator VESIM[2], as well as the simulation of the parallel HEV configuration (HE-VESIM)[3], both previously developed at the University of Michigan. HE-VESIM was configured in SIMULINK with the post-transmission electrical motor, lead-acid batteries, and a downsized diesel engine. It was utilized to assess the ability of advanced power management strategies to improve the fuel economy potential of the parallel HEV truck.[3] Even though previous experience with the HEV system simulation provided a good foundation for the current work, constructing a series hybrid system with eight in-hub motors required significant modifications of the system architecture. New, larger components as well as redefined power management strategy was also needed. In addition, the prospect of using the vehicle simulation within the target cascading optimization framework motivated implementation in the more computationally efficient software environment.

At the top level of the model hierarchy, SH-VESIM consists of the engine, battery, drivetrain, vehicle dynamics, and power control modules excited by the environment, as shown in Figure 3. A feed-forward simulation scheme is retained so as to enable studies of control strategies under realistic transient conditions. In other words, the first source of excitation comes from the driver who controls the vehicle velocity by means of the gas and brake pedals. Driver's command is translated by the Power Management Controller into signals defining operating parameters of the diesel engine, generator, and in-hub motors. The vehicle is constrained to move only on the pitch plane and has three degrees of freedom (longitudinal, heave, and pitch). The next excitation comes from the road that is usually uneven and imposes a velocity to the tires. Road excitation is applied to the four sets of tires as a function of their longitudinal position. Notice that the top-level model resembles the actual vehicle configuration. In contrast to previous efforts that relied on SIMULINK, the integrated vehicle model was developed using the 20SIM modeling and simulation environment.[4] The latter supports hierarchical structuring and allows the physical modeling by means

of bond graphs,[5, 6] block diagrams, or direct equation formulation. In addition, 20SIM allows the generation of stand-alone code, which is efficient for multiple evaluation of vehicle performance during design optimization.[7] The vehicle-level submodels in SH-VESIM are described next. The system-level suspension model is described at the end of this section.

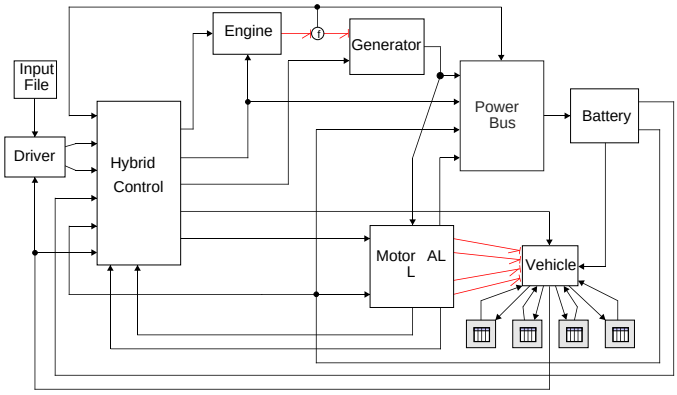

Figure 3. Vehicle model SH-VESIM as implemented in 20SIM

POWER SOURCES

Engine

High-fidelity thermodynamic models of in-cylinder processes and engine components have been developed to study powertrain transient response during vehicle acceleration.[2] On the other hand, a simplified but extremely fast engine module that utilizes torque look-up tables has been developed for system level studies of parallel hybrid-electric class VI trucks.[3] The latter approach was selected for this study since repeated simulation runs are needed for design optimization iterations, each one performed over a relatively long driving schedule. However, previous experience with high-fidelity modeling was used to add important additional features to the look-up-table based engine module in order to improve its dynamic response.

The high fidelity engine submodel is based on the parent phenomenological simulation presented in Reference 8, extensively validated for a variety of engine applications and extended to include transients in Reference 9. Results of studies published in Reference 2 illustrate the importance of high fidelity modeling of all turbocharged engine system components, including the fuel injection system, for accurate prediction of transient phenomena such as those occurring during the turbo-lag period. Although the objectives of the study presented here dictated the use of a simple engine submodel, it was deemed necessary to retain features critical for transient response. Namely, the engine module had to (a) incorporate a realistic fuel injection control module, and (b) include a delay function in the fuel injection controller to effectively simulate the turbo-lag associated with delayed response of the turbocharger and limited fueling during that period. Hence, the engine submodel was composed of two major parts: torque look-up table and fuel controller, as shown in Figure 4.

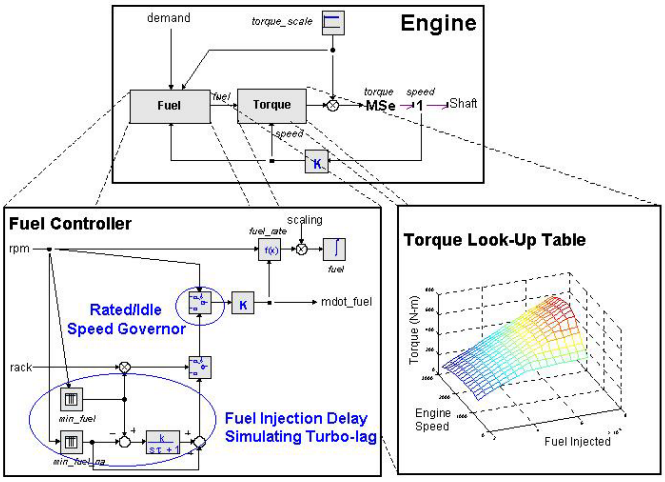

Figure 4. Engine submodel in 20SIM

The look-up table provides brake torque as a function of instantaneous engine speed and mass of fuel injected per cycle. A methodology for generating the torque map using the high fidelity simulation was developed and tested.[3] While engine testing is still used to calibrate model constants and validate its application to a specific engine design,[10, 11] the use of a simulation is beneficial in terms of facilitating easy scaling of the engine or evaluating new engine or component designs. In this study, the baseline look-up table is generated for a representative, modern, heavy-duty, in-line, six-cylinder, turbocharged, intercooled diesel engine. The specifications of baseline diesel engine manufactured by Detroit Diesel Corporation are listed in Table 1 of the Appendix. Engine rating roughly corresponds to the one used in the conventional powertrain, i.e. downsizing is avoided in order to prevent performance degradation in the series hybrid configuration. The relatively quiescent combustion chamber employs a shallow "Mexican hat" bowl-in piston and very high injection pressures, delivered by unit injectors. Fuel injection timing and duration are electrically controlled. The engine is set up for testing to support modeling and simulation activities at the W.E. Lay Automotive Laboratory of the University of Michigan.

The diesel engine fuel injection controller provides the signal for the mass of fuel injected per cycle based on driver demand, supplied by the driver module, and engine speed. Baseline fuel calibration is determined from engine dynamometer tests. At extreme speeds, the speed governor controls fuel injection mass to prevent the engine from stalling or over speeding. In addition, a carefully calibrated time delay is built-in to represent the effect of turbo-lag on transient response to rapid increases of engine "rack positions." The delay function affects only the portion of injected fuel dependant on availability of boost, and it is carefully tuned to match high fidelity predictions and observed system behavior during transient tests.[3, 11]

Battery

The battery submodel uses an electrical equivalent circuit to predict battery performance.[12] An advanced valve-regulated lead-acid (VRLA) battery with 18Ah module capacity is chosen as the baseline battery model. The battery internal resistance and the open circuit voltage are functions of battery state of charge (SOC), as shown in Figure 5 based on data from Reference 13. It should be noted that discharging efficiency decreases toward the smaller SOC range and charging efficiency decreases toward the higher SOC range. Delivering more power in driving and absorbing more power in deceleration can be achieved by increasing the total number of battery modules. However, packing size and weight of the battery may degrade vehicle performance due to low power density.

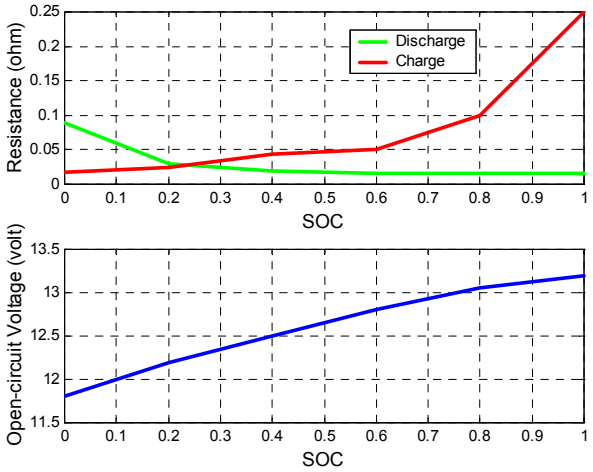

Figure 5. Battery resistance and open-circuit voltage

DRIVETRAIN

The drivetrain submodel consists of the generator and its gearbox, power bus, and four sets of in-hub motors with a gearbox (Figure 6). The drivetrain provides the connection between the engine and the vehicle dynamics. The generator gearbox input shaft and in-hub motor gearboxes are the connecting points for the engine and vehicle dynamics models, respectively. The inputs are the engine torque and wheel rotational speed, and the outputs are the torque to the wheels, generator rotational speed and battery power. The in-hub motors, generator, and batteries are connected to the power bus that controls the power flow between these electrical components. The power flow is controlled by the power control module (more details are given in the Power Management section).

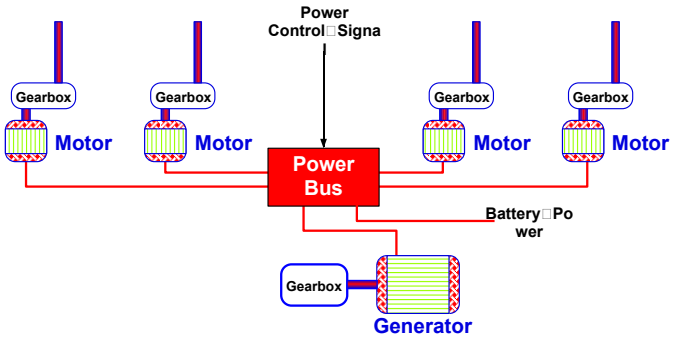

Figure 6. Drivetrain configuration

Motor

An 83 kW AC induction motor is selected as the baseline electric motor. Efficiency is a function of motor torque and motor speed, i.e., $\eta_m = f(T_m, \omega_m)$. The efficiency map used in this study was adopted from the ADVISOR library[13] and is shown in Figure 7. Motor dynamics are approximated by a first-order lag. However, motor torque output is limited due to the battery maximum power and motor maximum torque limits.

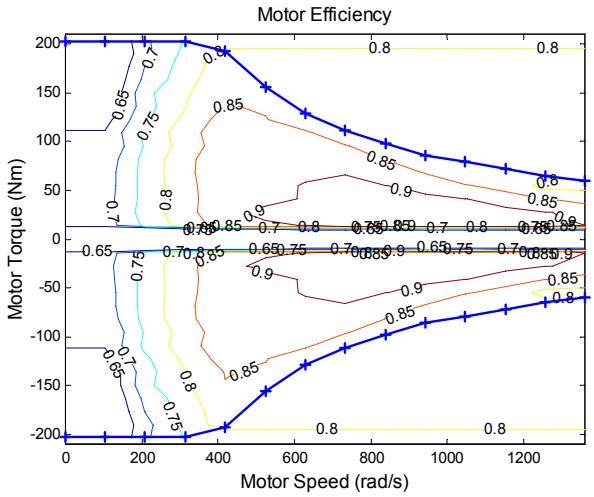

Figure 7. AC induction motor efficiency

Generator

The generator is connected to the diesel engine via a speed reduction gearbox to transform mechanical into electrical power. This engine and generator combination is referred to as power generating unit (PGU). A 350 kW generator is chosen to match the baseline diesel engine. The generator model includes torque and speed dependent efficiency data, as shown in Figure 8. Generator inertia was combined with engine inertia to enable solution of PGU dynamics. Both engine and generator efficiency must be taken into account to optimize the PGU operation, as described in the Power Management section.

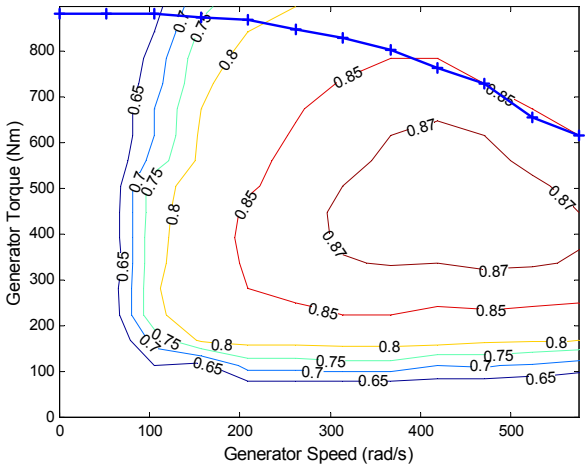

Figure 8. Generator efficiency

VEHICLE DYNAMICS

The vehicle dynamics submodel considers the wheels, tires, axles, suspensions, and frame of the vehicle. The vehicle is modeled as a collection of rigid bodies that are allowed to move in the 2-dimensional space subject to forces, moments and rigid constraints (Figure 9). Forces and moments are physical elements that act at specific points of two bodies, e.g., the suspension force between the wheel hub and the attachment point on the frame. In addition, two bodies can be restrained to move in a specific trajectory by a rigid constraint, e.g., the front axle is constrained to move perpendicular to the frame.

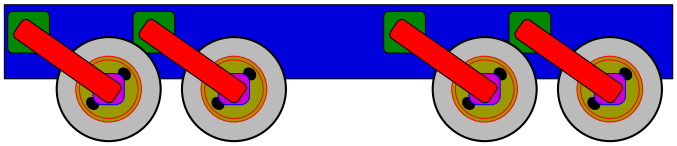

Figure 9. Half car model

The frame is modeled as a rigid body that is free to move horizontally and vertically, and to pitch. Three inertial elements are used to represent the dynamics in three degrees of freedom. The kinematics are described in a body fixed frame and represented by the nonlinear Euler equations. Gravity force is applied at the center of gravity (CG) after transforming the CG velocity in the inertial frame. This is a standard coordinate transformation around the out of plane axis. The frame includes four points for connecting the axles at fixed locations relative to the CG. Finally, aerodynamic drag is modeled by energy losses that are quadratic with the forward vehicle velocity.

Each axle is modeled as a rigid body with its kinematics described in a body fixed frame (x, y) (Figure 10). The axle is constrained by a rigid constraint to move on an axis that has its origin at the attachment point (p^i) and is perpendicular to the horizontal axis of the frame (x^i, y^i). The axle is also constrained by the suspension that is modeled as a linear spring and damper connected in parallel. Finally, gravity force is applied to the axle through a transformation of local velocities into the global frame (X, Y).

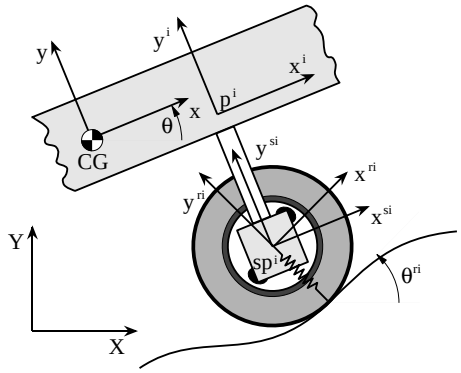

Figure 10. Tire and suspension kinematics

The tire submodel includes the wheel dynamics and the interaction of the tire with the road. Wheel mass is lumped to the axle to avoid more kinematic constraints and computational inefficiencies. The model includes the wheel moment of inertia and bearing viscous losses at the wheel hub. Drive torque from the drivetrain is applied to the hub to accelerate the wheel. A simple brake model with viscous and coulomb friction is included to generate the required torque for decelerating and stopping the vehicle. Tire rolling resistance is added to the model as an additional source of energy loss.

Tire forces in the vertical direction are modeled as a linear spring and damper connected in parallel. The model can also predict wheel lift off. The longitudinal traction force is calculated using the Pacejka model taken from Reference 14. First, the axle velocity at point (sp^i) is converted in a frame that is aligned with the road at the contact point. This coordinate transformation gives the forward velocities of the contact point (sp^i in the (x^{ri}, y^{ri}) frame) that is used to calculate wheel slip. Finally, traction force is calculated as a nonlinear function of wheel slip and normal load. The constants in the Pacejka model are estimated from measured data of the actual tire.

POWER MANAGEMENT

The power management strategy is based on engineering intuition and simple analysis of component efficiencies.[3, 15] The power management process starts by interpreting the driver pedal signal as a power request P_{req}. According to the power request, the operation of this controller is divided into three control modes: Braking, Normal and Recharging. If the power request is negative, Braking mode is engaged to decelerate the vehicle. If the power request is positive, either Normal mode or Recharging modes are used according to a charge-sustaining policy. The charge-sustaining strategy assures that the battery state of

charge (SOC) stays within preset lower and upper bounds for efficient operation and prevention of battery depletion or damage. In a normal propulsive driving condition, the Normal mode control determines the power flow in the series hybrid drivetrain. Whenever the SOC drops below the lower limit, the controller will switch to the Recharging mode until the SOC reaches the upper limit, and then Normal mode will resume. The basic logic of each control mode is briefly described below.

Normal Mode

The battery is the prime power source in this mode. The PGU (engine and generator) is shut off and the battery supplies the requested power to the electric in-hub motor. However, once the power request exceeds what the battery can generate, the engine is turned on to supply the additional power.

Charging Mode

The PGU is the prime power source in this mode. In addition to powering the electric motor, the PGU has to provide additional power to charge the battery. A constant recharge power level P_{ch} is added to the PGU's power request.

$$P_{pgu} = P_{req} + P_{ch} \quad ,$$

where $P_{ch} = \alpha \cdot P_{bat\_\max}$ and α is the fraction of battery charging power limit. The battery power command becomes negative to recharge the battery. One exception is when the total power request is greater than the maximum PGU power; in this case, the battery will assist the PGU to power the electric motor. Once the PGU power request is determined, the desired engine torque and speed can be found from the curve shown in Figure 11. This curve is calculated by combining engine and generator efficiencies, and represents the most efficient operating points for each engine power level.

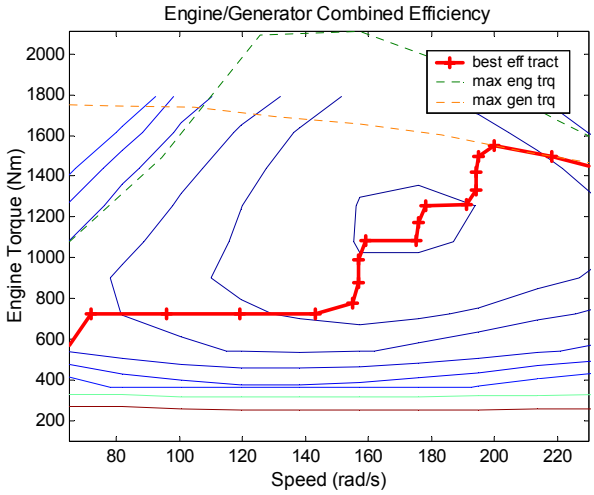

Figure 11. Best PGU efficiency curve

Braking Mode

A driver's stepping on the brake pedal is interpreted as a negative power request. Regenerative braking is activated to absorb braking power. However, when the braking power request exceeds the regenerative braking capacity due to battery or motor limits, friction braking is activated to produce vehicle deceleration.

SUSPENSION SYSTEM MODEL

A detailed model of the suspension is needed for predicting the equivalent stiffness and damping parameters that are passed to the upper vehicle level from the lower system level of the target cascading hierarchy. The suspension has a trailing arm that houses two hydraulic chambers (C_1 and C_2) and a pneumatic chamber (C_3), as shown in Figure 12. The swinging motion of the arm around the pivot point O moves the piston that compresses the fluid in chamber C_3 after the hydraulic fluid is forced to pass through the orifice. This mechanism provides the stiffness characteristics, while the fluid flow through the orifice of area A_{12} provides viscous energy losses with hysteretic effects. Stiffness and damping characteristics are calculated using the nonlinear kinematics of the trailing arm, which depend on the geometry and fluid properties. The quantities that are variables in the system-level design problem are:

- High pressure piston Area, A_S
- Low pressure piston Area, A_P
- Orifice area, A_{12}
- Wheel hub location, L_H
- Rod hitch point, X_3
- Rod hitch point, Y_3
- Rod length, L_R
- Trailing angle, α

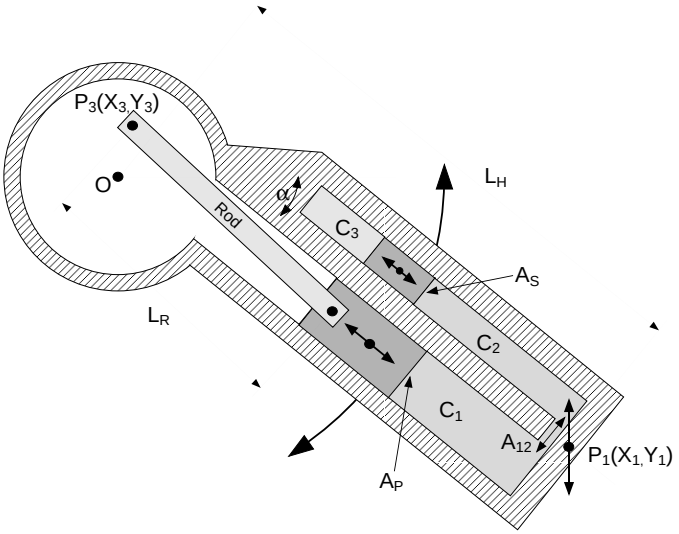

Figure 12. Trailing arm suspension

IMPLEMENTATION

The coordination and information flow of the analytical target cascading process is illustrated in Figure 13. Targets and responses are shown in octagons, design variables are shown in diamonds, optimizers are shown in rectangles, and analysis models are shown in ovals.

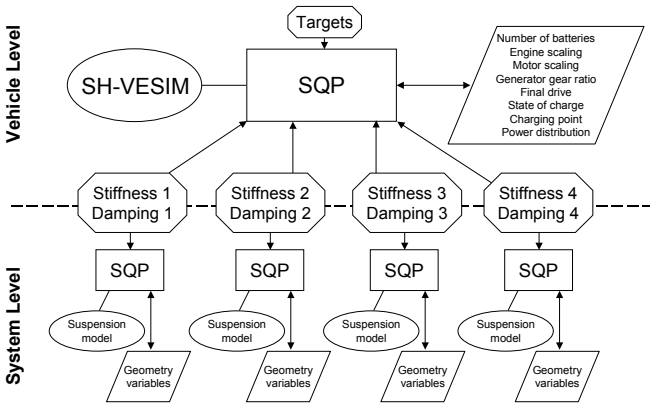

Figure 13. Coordination and information flow of the analytical target cascading process for the case study

The vehicle-level problem is solved first: Truck design targets are set for improving fuel economy, performance, and ride quality. Design variables include engine and motor size, number of battery modules, generator gearbox ratio, final drive, state of charge limits, battery charging point, and power distribution ratios. System responses consist of damping and stiffness characteristics for the four different suspensions. It is emphasized that system responses are treated as optimization variables at the vehicle level. The Sequential Quadratic Programming (SQP) algorithm implementation of the MATLAB Optimization Toolbox[16] was used as the optimizer for both vehicle- and system-level problems.

Once system response values have been determined by solving the vehicle-level problem, they are cascaded down to the system level, where four problems are solved independently to match them. Design variables for the four system-level problems consist of the suspension geometric variables. After solving the system-level problems, the updated response values are passed up to the upper level, where the vehicle-level design problem is solved again. If response matching is not satisfactory the whole process is repeated in an iterative manner until convergence within some tolerance is achieved.

DRIVING SCENARIO

A combined driving scenario was generated for evaluation of vehicle mobility, performance, and fuel economy. The velocity time history and road profile were created based on the driving requirements given in Table 2 of the Appendix. The uneven road profile is needed for the accurate evaluation of ride quality (absorbed power) at the driver's seat. Vehicle performance is evaluated as it is riding over a network of roads with different harshness characteristics. The network consists of four sections that represent rough trails, trails, secondary roads, and primary roads. Vehicle velocity is adjusted to represent realistic driving conditions (Figure 14). Road elevation is generated to represent the statistical description of each section, as shown in Figure 15.

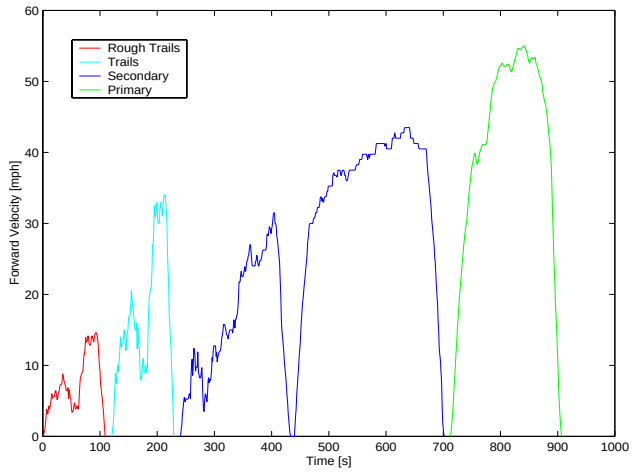

Figure 14. Driving cycle

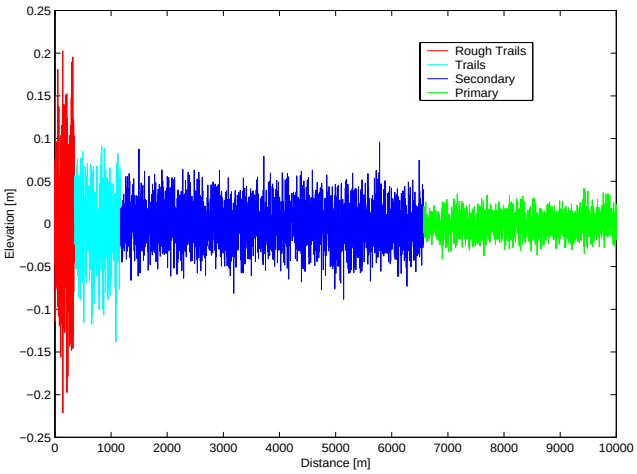

Figure 15. Road profile

STATE OF CHARGE CORRECTION

The maximum and minimum state of charge limits are treated as design variables at the vehicle level. Matching initial and final state of charge is necessary to ensure a fair comparison of fuel efficiency among different truck designs. This is achieved by forcing the simulation to continue when the state of charge at the end of the driving cycle is less than the initial one, which is set to the maximum limit. In this case, the engine runs on idle and recharges the batteries; the simulation stops when the starting state of charge has been reached. Figure 16 depicts an example that illustrates the process described above.

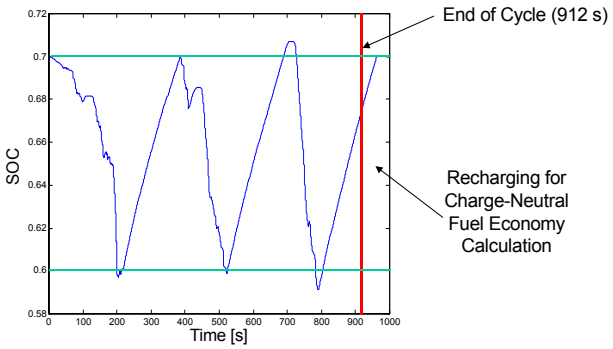

Figure 16. State of charge correction

PROPULSION SYSTEMS

Two different propulsion system configurations were considered in the case study: a series hybrid and an electric drive. The electric drive configuration does not use the batteries as the power source. Thus, design variables at the vehicle level do not include number of battery modules, state of charge limits, and charging point for the electric drive configuration. Results are presented for both configurations and conclusions are drawn in regard to which propulsion system should be preferred in the design.

TRUCK DESIGN TARGETS

Two sets of targets were used for this concept truck design study. In the first part of the study, the goal was to achieve a fuel efficiency that would be better by at least 50 percent than the one of the Heavy Expanded Mobility Tactical Truck (HEMTT). Fuel economy was computed at both the Gross Vehicle Weight (GVW, truck weight plus payload, 22,977 kg) and the Gross Combined Vehicle Weight (GCVW, GVW plus trailer, 38,886 kg). Performance metrics were to be maintained at the same levels of those of the HEMTT. These included maximum speed on flat road at GVW and maximum speed on 2 percent grade at GCVW, both without use of batteries. As part of the evaluation of the performance of the truck, it was required that the maximum speed degradation at GCVW on flat road be not more than 20 percent compared to the speed at GVW. Ride quality, measured as absorbed power at the driver's seat, was to be kept at 10 percent of the maximum value allowed for the HEMTT at GVW.

In the second part of the study, specific numerical values were not defined as targets; instead, it was attempted to improve all metrics as much as possible. Numerical values of the targets and the actually achieved truck responses are summarized in Tables 3 and 4 of the Appendix for the two different sets of targets. The results are presented and discussed in more detail in the next section.

RESULTS AND DISCUSSION

Attributes of interest for both the series hybrid and the electric drive are compared in Figure 17 for the first set of targets. Results are normalized such that 1.0 represents the target values. It can be seen that the first three targets are achieved. It should be noted that the target for maximum speed on flat road at GVW was already achieved by the baseline design. The last three responses are improved compared to the baseline design but do not achieve the targets. The maximum speed degradation for the series hybrid configuration comes very close to the target. Note that responses that achieve or exceed their targets become "neutral" to the optimizer, i.e., they do not contribute to the objective function.

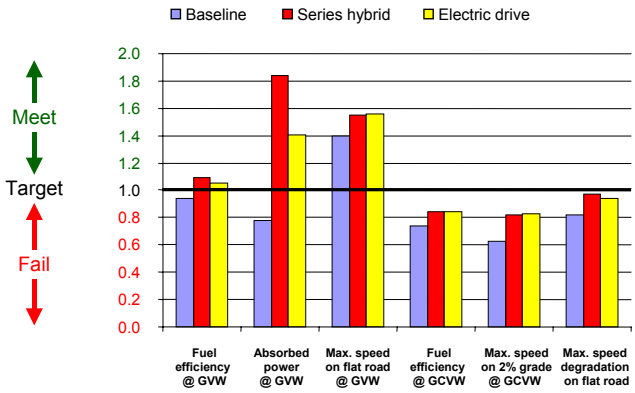

Figure 17. Achievement of specific targets

In summary, responses estimated for GVW achieve their targets, while responses estimated for GCVW do not. Hence, it appears that performance targets at GCVW were too stringent. Results obtained for GCVW indicate a possible trade-off between conflicting targets, i.e., it seems that the performance targets prevent more substantial improvement of the fuel economy attribute. Nevertheless, both configurations of the advanced truck demonstrate better fuel economy than baseline design, with the series hybrid configuration being slightly superior to the electric drive, while they both demonstrate similar performance improvements. One explanation for less than optimal overall vehicle performance at GCVW is the use of affordable, but certainly not high end electrical components; e.g., replacement of lead-acid batteries with more advanced counterparts would lead to improved system behavior.

The same trend is observed for the second set of targets presented in Figure 18. Results are normalized with respect to the first set of targets for the sake of comparison. Note that in this case the optimizer tries to improve all responses as much as possible without limits. This leads to a dramatic increase of the ride quality. Hybrid vehicle fuel economy shows more modest, but tangible further improvements over the conventional at both GVW and GCVW, the actual fuel economy gains being 17.4 percent and 15.6 percent compared to the baseline design, respectively. At the same time performance metrics of the hybrid are maintained at about the same level as in the previous study conducted with specific targets. For the electric drive propulsion system only the ride quality displays significant further improvement compared to the optimization performed for the specific targets, while all other responses remain about the same.

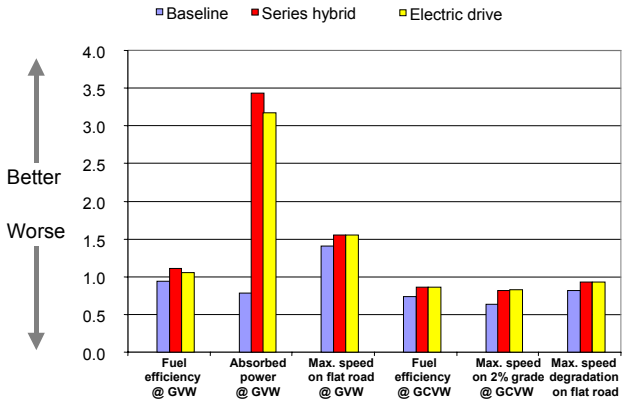

Figure 18. Achievement of maximal improvement targets

Two sets of results are presented in Tables 3 and 4 of the Appendix for the specific and maximal improvement targets, respectively. These tables include relative improvement of the vehicle responses with respect to the baseline values. Final design variable values and suspension responses are compared to the baseline design values in Table 5 of the Appendix for series hybrid configuration and maximal improvement targets.

SUMMARY AND CONCLUSIONS

The target cascading methodology has been successfully applied for conceptual design of an advanced heavy tactical truck. Two levels, i.e., vehicle and system levels were considered. At the vehicle level, all necessary models were developed to represent the truck, and design variables were determined to satisfy two different sets of targets. Both a series hybrid and an electric drive configuration were considered as propulsion systems. At the system level, a variable height suspension system was modeled, and specifications were obtained for four independent systems corresponding to the four axles of the truck. Given the stringent performance targets, the driving cycle, and the low efficiency of electrical components, the series hybrid configuration proved to be slightly superior.

It can be concluded that target cascading is useful and can be used to avoid costly design iterations late in the product development process, help identify and evaluate trade-off relations between conflicting targets, and obtain a final design that is consistent by means of coordination of cascaded responses.

ACKNOWLEDGMENTS

The authors would like to acknowledge the technical and financial support of the Automotive Research Center (ARC) by the National Automotive Center (NAC), U.S. Army Tank-Automotive Research, Development and Engineering Center (TARDEC), and thank Walter Bryzik, David Gorsich, and Nance Halle for their help and guidance. The ARC is a U.S. Army Center of Excellence for Automotive Research at the University of Michigan, currently in partnership with the University of Alaska-Fairbanks, Clemson University, University of Iowa, Oakland University, University of Tennessee, Wayne State University, and University of Wisconsin-Madison.

REFERENCES

1. Kim, H.M., Michelena, N.F., Papalambros, P.Y., and Jiang, T., 2000. Target Cascading in Optimal System Design. Proceedings of the 2000 ASME Design Automation Conference. Paper No. DAC-14265. Baltimore, Maryland, USA
2. Assanis, D.N., Filipi, Z.S., Gravante, S., Grohnke, D., Gui, X., Louca, L.S., Rideout, G.D., Stein, J.L., and Wang, Y., 2000. Validation and Use of SIMULINK Integrated, High Fidelity, Engine-In-Vehicle Simulation of the International Class VI Truck. SAE Paper 2000-01-0288, SAE 2000 World Congress
3. Lin, C-C, Filipi, Z., Wang, Y., Louca, L., Peng, H., Assanis, D., and Stein, J., 2001. Integrated, Feed-Forward Hybrid Electric Vehicle Simulation in SIMULINK and its Use for Power Management Studies, SAE Paper 2001-01-1334
4. 20SIM, 2001. 20SIM Pro Users' Manual, Version 3.2. The University of Twente - Controllab Products B.V. Enschede, The Netherlands
5. Rosenberg, R.C., and Karnopp, D.C., 1983. Introduction to Physical System Dynamics. McGraw-Hill, New York, NY
6. Karnopp, D.C., Margolis, D.L., and Rosenberg, R.C., 1990. System Dynamics: A Unified Approach. Wiley-Interscience, New York, NY
7. Louca, L.S., Stein, J.L., and Rideout, D.G., 2001. Integrated Proper Vehicle Modeling and Simulation Using a Bond Graph Formulation. Proceedings of the 2001 International Conference on Bond Graph Modeling. Phoenix, AZ. Published by the Society for Computer Simulation, ISBN 1-56555-221-0, San Diego, CA
8. Assanis D.N., and Heywood J.B., 1986. Development and Use of a Computer Simulation of the Turbocompounded Diesel System for Engine Performance and Component Heat Transfer Studies," SAE Paper 860329
9. Filipi, Z.S. and Assanis, D.N., 1999. A Non-linear, Transient, Single-Cylinder Diesel Engine Simulation for Predictions of Instantaneous Engine Speed and Torque. ASME Journal of Engineering for Gas Turbines and Power, volume 123, issue 4; also presented at the ASME 1997 ICE Spring Technical Conference, Fort Collins, CO
10. Assanis, D.N., Atreya, A., Borgnakke, C., Dowling, D.R., Filipi, Z.S., Hoffman, S., Homsy, S., Kanafani, F., Morrison, K., Patterson, D., Syrimis, M., Winton, D., Zhang G., and Bryzik, W., 1997. Development of a Modular, Transient, Multi-Cylinder Diesel Engine Simulation for System Performance and Vibration Studies. Proceedings of ASME-ICE Spring Technical Conference, Vol. 28-1, Fort Collins, CO, pp. 87-101
11. Assanis, D.N., Filipi, Z.S., Fiveland, S.B., and Syrimis, M., 2000. A Methodology for Cycle-By-Cycle Transient Heat Release Analysis in a Turbocharged Direct Injection Diesel Engine. SAE Special Publication Series volume SP- 1530 (considered for inclusion in 2000 SAE Transactions, Journal of Engines), presented as SAE paper 2000-01-1185 at the 2000 SAE International Congress, Warrendale, PA
12. Wiegman, H.L.N. and Vandenput, A.J.A., 1998. Battery State Control Techniques for Charge Sustaining Applications. SAE Paper 981129
13. Brooker, A., Hendricks, T., Johnson, A, Kelly, K., Markel, T., O'Keefe, M., Sprik, S., and Wipke, K., 2000. ADVISOR 3.0 Documentation. National Renewable Energy Laboratory
14. Pacejka, H.B. and Bakker, E., 1993. Tyre Models for Vehicle Dynamics Analysis. Proceedings of the 1st International Colloquium on Tyre Models for Vehicle Dynamics Analysis. Delft, Netherlands
15. Anderson, C., and Pettit, E., 1995. The Effects of APU Characteristics on the Design of Hybrid Control Strategies for Hybrid Electric Vehicles. SAE Paper 950493
16. Coleman, T., Branch, M.A., and Grace, A., 1999. Optimization Toolbox for Use with MATLAB, User's Guide. The MathWorks, Inc., Natick, MA

APPENDIX

Table 1. DI Diesel engine specification

Configuration	V6, Turbocharged, Intercooled
Displacement [l]	12.7
Bore [cm]	13.0
Stroke [cm]	16.0
Con. rod length [cm]	26.93
Compression ratio [-]	15.0
Rated power [kW]	350 @ 2100 rpm

Table 2. Driving scenario characteristics

Road Type	Distribution [%]		Elevation RMS [m]	Average Speed [mph]
	Time	Distance		
Rough Trails	**15**	**5**	**0.068**	**8**
Trails	**15**	**10**	**0.040**	**17**
Secondary Road	**50**	**50**	**0.025**	**26**
Primary Road	**20**	**35**	**0.013**	**40**

Table 3. Achievement of specific targets

Response	Base-line	Tar-get	Series hybrid		Electric	
			value	impr.	value	impr.
Fuel economy at GVW [mpg]	3.68	3.9	4.25	15.7 %	4.1	11.5 %
Absorbed power at GVW [W]	0.64	0.5	0.27	57.7 %	0.36	44.8 %
Maximum speed at GVW on flat road [mph]	77	55	85.45	11.0 %	85.6	11.2 %
Fuel economy at GCVW [mpg]	2.15	2.3	2.44	13.6 %	2.45	14.4 %
Maximum speed at GVW on 2% grade	31.5	50	40.76	29.4 %	41.5	31.7 %
Maximum speed degradation on flat road [%]	24.3	20	20.6	15.3 %	21.3	12.6 %

Table 4. Achievement of maximal improvement targets

Response	Base-line	Tar-get	Series hybrid		Electric	
			value	impr.	value	impr.
Fuel economy at GVW [mpg]	3.68	∞	4.32	17.4 %	4.13	12.5 %
Absorbed power at GVW [W]	0.64	0	0.15	77.3 %	0.16	75.6 %
Maximum speed at GVW on flat road [mph]	77	∞	85.33	10.8 %	85.6	11.2 %
Fuel economy at GCVW [mpg]	2.15	∞	2.48	15.6 %	2.49	15.8 %
Maximum speed at GVW on 2% grade	31.5	∞	40.86	29.7 %	41.43	31.5 %
Maximum speed degradation on flat road [%]	24.3	0	21.55	11.5 %	21.54	11.6 %

Table 5. Baseline and final designs and suspension responses for series hybrid configuration and maximal improvement targets

	Baseline value	Final value
Truck design variables		
Number of battery modules [-]	120	160
Motor scaling [-]	1.0	1.24
Engine scaling [-]	1.0	1.25
Low SOC limit [-]	0.6	0.72
High SOC limit [-]	0.7	0.82
Generator gear ratio [-]	2.0	2.32
Final drive [-]	15	27.78
Battery charging point [-]	0.8	0.62
Power distribution, axle 1 [%]	25	26
Power distribution, axle 2 [%]	25	24
Power distribution, axle 3 [%]	25	24
Power distribution, axle 4 [%]	25	26
Suspension responses		
Stiffness, axle 1 [N/m]	500,000	333,333
Damping, axle 1 [Ns/m]	10,000	15,000
Stiffness, axle 2 [N/m]	500,000	333,333
Damping, axle 2 [Ns/m]	10,000	15,000
Stiffness, axle 3 [N/m]	500,000	714,285
Damping, axle 3 [Ns/m]	10,000	15,000
Stiffness, axle 4 [N/m]	500,000	333,333
Damping, axle 4 [Ns/m]	10,000	15,000

Suspension design variables					
	Base-line	Final			
		Axle 1	Axle 2	Axle 3	Axle 4
High pres. area [m^2]	0.02	0.015	0.015	0.0045	0.015
Low pres. area [m^2]	0.05	0.037	0.037	0.0068	0.037
Orifice area [m^2]	0.01	0.012	0.012	0.0034	0.012
Wheel hub loc. [m]	0.6	0.4	0.4	0.4	0.4
X_3-coordinate [m]	0.0	0.105	0.105	0.15	0.105
Y_3-coordinate [m]	0.1	0.106	0.106	0.0	0.106
Rod length [m]	0.5	0.36	0.36	0.22	0.36
Trailing angle [rad]	0.7854	0.7854	0.7854	0.7854	0.7854